Tomographic Estimation of Shear Velocities from Shallow Cross-Well Seismic Data

BG4.5

William S. Harlan, Conoco Inc.

SUMMARY

A cross-well, shear-wave data set posed two problems: 1) wells are separated by only 12.5 wavelengths, so thin raypaths are a poor approximation; 2) data are recorded through a high-velocity limestone surrounded by low-velocity shales. Waves are bent considerably, so either refracted or direct arrivals can arrive first. Only first-arrivals can be picked with any reliability.

Ray tracing is avoided entirely by extrapolating traveltimes explicitly from sources or receivers to every point in a region of interest. Rather than search for a single fastest raypath, this method finds Fresnel regions containing all paths that add constructively to first-arrivals. This method also robustly finds minimum traveltimes, whether direct or refracted.

The resolution of the estimated velocity model is controlled explicitly with basis functions of adjustable width. Wavepaths and velocities are estimated alternately: as the accuracy of paths improves, velocities are allowed to introduce sharper detail. No more two-dimensional detail is introduced than necessary.

INTRODUCTION

Like velocity analysis, traveltime tomography estimates a velocity model that explains the arrival times and moveouts of coherent arrivals. Traveltime tomography is most sensitive to smooth background changes in transmission velocities--those changes which must be known for depth migration or diffraction tomography.

Current methods of seismic traveltime tomography use a variety of methods described as "ray-tracing" or "ray-shooting." These methods invoke Snell's law at boundaries of cells of constant velocity (Langen et al., 1985, offer improvements) or dynamically extrapolate differential ray equations (e.g., Wesson, 1971). Other alternatives include relaxation methods (e.g., Aki and Richards, 1980). Berryman, 1989, constrains raypaths as a sum of low-order sinusoids and minimizes traveltimes with a simplex search algorithm. Van Trier and Symes, 1990, recently proposed applying perturbation theory directly to finite-difference extrapolations of the Eikonal equation.

All these methods assume asymptotically infinite frequencies in the source, and by implication, infinitely thin raypaths. However, frequency content can limit tomographic resolution more drastically than angular coverage. Woodward, 1989, has built on the work of Hagedoorn, 1954, to replace raypaths in tomography by "band-limited raypaths" or "wavepaths."

With new explicit schemes (e.g., Moser, 1989) we can extrapolate traveltimes from sources or receivers to every point in a region of interest. Rather than search for a single fastest raypath, we can find Fresnel regions containing all paths that add constructively to first-arrivals. This approach robustly finds minimum traveltimes, whether direct or refracted, in complicated media with large velocity contrasts.

The velocity model can be constrained as a sum of smooth basis functions of adjustable width in all dimensions (cf. Harlan, 1989). As alternately reestimated wavepaths and velocities improve, the resolution of the velocity model can be allowed to increase--first vertically, then over all dimensions. The result is the smoothest, most stratified velocity model that explains the data.

A DESCRIPTION OF THE DATA

The cross-well data used in this report were recorded in 1989 at the Conoco Borehole Test Facility. A source provided a rotary motion in one well while three-component accelerometers recorded the transmitted motion in a well 88.6 m away. Two directions of rotary motion were later decomposed into inline compressional motion and cross-line shear motion.

Figure 1 shows a compressional (sonic) velocity log for the well containing receivers. This log shows the high velocity of the Ft. Riley limestone, which ranges from 15 m to 30 m in depth. An overlying limestone, approximately 2 m thick, is narrower than the shortest spatial wavelength and cannot carry significant refracted energy. Surrounding shales have less than half the velocity of the limestones.

Figure 2 shows a typical shear-wave gather for a common receiver at 38.3 m depth. 63 traces, from left to right, correspond to increasing source depths from 3.0 m to 40.8 m. 10 fixed receivers ranged from 9.1 m to 42.0 m depth. Deconvolution of the recorded source waveform has compressed the data into 100 ms with a bandwidth of 70 - 280 Hz. Shear data has twice the resolution of compressional data.

Only first arrivals can be picked and correlated with some confidence. The flat central arrivals correspond to source positions in the high-velocity Ft. Riley limestone (approximately 2000 m/s). Low-velocity shales produce steep events. The slight ringing of waveforms has been modeled elastically as a sequence of many overlapping arrivals. At 280 Hz we would expect a 7.6 m spatial wavelength in the limestone and less than half this length in shales.

Figure 3 shows a model of fastest paths between every third shot (left) and all available receivers (right). The stratified shear velocity model (not logged directly) was proposed by a geologist from other available information. Notice that all paths pass through the limestones; large regions of the shales receive no coverage at all. Also, the angles of paths through the limestone do not vary as much as would the angles of straight lines.

These plotted "wavepaths" required numerical tools that addressed two problems. 1) Wells are separated by only 12.5 wavelengths, so thin raypaths are a poor approximation. 2) Waves are bent considerably, so either refracted or direct arrivals can arrive first.

TRACING WAVEPATHS

According to Huygen's principle, wave energy effectively travels along all possible paths between two points, including those that ignore Snell's law. In the optical approximation (infinite frequencies), however, all significant contributions of energy follow paths that obey Fermat's principle and locally minimize the traveltime.

On the other hand, band-limited waves can follow paths that are not Fermat raypaths and still cover the distance between two points in almost the same time. All arriving waves that are delayed by less than half a wavelength will add constructively to the first arrival. These data have a minimum temporal wavelength of 3.6 ms; thus, any waves that arrive in less than 1 ms of each other will be indistinguishable. Errors in picking first-arrival times will be even greater.

Figure 4 shows a gray region that contains many possible paths between a shallow source and a deep receiver. Each of these paths has a total traveltime no more than 1 ms greater than the minimum possible traveltime, according to the geologist's velocity model. Three plotted lines show a central "median" path and the approximate half-width of this region. The gray region bends sharply at the edge of the high-velocity layer and then broadens. High velocities allow greater variations in the path because these variations affect traveltimes less.

Wave paths were calculated with a new, but simple numerical algorithm:

1. With an explicit scheme, extrapolate minimum traveltimes from one source position to each point in the region of interest. Explicit schemes include finite-difference extrapolation of the Eikonal equation (Vidale, 1989), or the "graph theory" method of Moser, 1989 (which I use). Similarly, extrapolate traveltimes from one receiver location to each point in the region of interest.
2. Add together the extrapolated traveltimes from source and receiver. The resulting table shows the traveltimes of paths which are obliged to pass through particular points in the model. The global minimum traveltime of this table is the minimum traveltime between the source and receiver. This minimum is realized at both the source and receiver locations and also at each point along the Fermat raypath with global minimum traveltime.
3. Find all points in the model whose tabulated traveltimes exceed the minimum traveltime by less than half a temporal wavelength. This region will be called the wave path of the first arrival. A smooth path that passes through the center of this region has a traveltime that differs little from that of the Fermat raypath. This representative "median" path will later be used for modeling traveltimes and tomographically improving velocities. The variable width of the path can be preserved as well.

CHOOSING PARAMETERS FOR VELOCITIES

Let us find the smoothest, most horizontally stratified velocity model possible to explain picked traveltimes. The resolution of inverted velocities will be limited by source bandwidth, by the distribution of our measurements, and by errors in the positioning of wave paths. We should add sharper details (higher spatial frequencies) to the velocity model only if smoother models will not explain the data. Also, in such a geologically stratified region as at the Borehole Test Facility, we should not add more two-dimensional complexity than necessary. Since many possible models may explain the data equally well, let us choose the simplest, both mathematically and geologically.

To control the resolution of the model, I constrain slowness, the reciprocal of velocity, as a sum of smooth basis functions. The widths of these basis functions can be narrowed as wave paths are improved, allowing sharper changes in velocities. Slowness will be more convenient to evaluate than velocity because traveltime is an integration of slowness along the length of a path.

If s_{ij} represents the slownesses of node points, then the slowness at spatial coordinates x and z will be

$$s(x,z) = \sum_i \sum_j s_{ij}\, dx^{-1}\, dz^{-1}\, f[(x - i\,dx)/dx]\, f[(z - j\,dz)/dz].$$

dx and dz are the spatial sampling rates of the nodes. f(x) represents a bell-curve of unit area and unit width, such as a Gaussian or third-order polynomial.

To improve a particular slowness model, we should constrain the perturbations with an appropriate density of basis functions, depending on the accuracy and width of estimated wave paths. Optimized perturbations can then be added to a gridded reference slowness model of fixed sampling (60 by 60 for these data). Alternating improvements in paths and slownesses will allow an increasing density of basis functions.

ITERATIVE OPTIMIZATION

Let us begin with the simplest possible model: 1) assume that paths are straight lines, and 2) assume a single average slowness. First, I constrain the slowness perturbation with only three basis functions over depth and with no lateral variation at all.

I minimize errors between picked and modeled first-arrival times by optimizing slowness perturbations with a conjugate-gradient algorithm (Luenberger, 1984; Scales, 1987). This algorithm requires that we alternately perform forward modeling and its numerically adjoint operation, backprojection. Forward modeling links two steps: 1) gridding smooth slowness values from basis functions, and 2) integrating traveltimes from slownesses along known paths. Both operations are linear. The adjoint reverses these steps: 1) perturb slownesses along the paths with values proportional to errors in traveltime, and 2) find perturbations of basis functions from weighted sums of gridded values.

Figure 5 shows the first revised velocity model and reestimated wavepaths, which have been drastically repositioned towards the higher velocity center. Each succeeding reestimate of velocities allowed an increasing number of vertically variable basis functions (up to 25) until an optimal one-dimensional solution was obtained. Then, beginning again with smooth perturbations, a two-dimensionally variable velocity function was optimized (Figure 6).

The bottom of the Ft. Riley is positioned as expected, but no thin shallow limestone appears above 15 m depth. Shallow velocities are much slower than expected. Modeled traveltimes had an error less than 1.8 ms -- within one temporal wavelength and the expected picking error. This model fits the picked data only 0.2 ms better than the entirely stratified model. If we had directly optimized a two-dimensional velocity model, we would see the imprint of an hour-glass-shaped distribution of raypaths. Instead, the stratified model has extrapolated reasonable velocities into regions not covered by first-arrivals.

CONCLUSIONS

Estimated shear velocities from Conoco's cross-well data showed vertical resolution of approximately 3 m for a 70-280 Hz

bandwidth. Estimated lateral changes were insignificant, as expected in this geologically stratified area. An entirely stratified model explained the picked traveltimes to within the picking error.

Because of large velocity contrasts, first-arriving waves did not pass through large regions of low-velocity shales. The margins, but not interiors, of these shales were resolvable from neighboring refractions. Only the interior of a high-velocity limestone received much angular coverage. Geologic layers did not carry any detectable refracted waves when thinner than the shortest seismic wavelength.

The estimated interval velocity function extrapolated reasonable values into regions of poor ray coverage by converging first on the long spatial wavelengths and by encouraging stratification. Estimated wavepaths guide our interpretation of nonuniqueness and resolution.

ACKNOWLEDGEMENTS

None of this work would have been possible without Conoco's Experimental Group of Worldwide Exploration. John Queen worked closely with the author at all stages of the project. Jack Cole designed the seismic source, and Dale Cox devised the necessary multicomponent waveform processing. Discussions with Doug Hanson and Shein Wang were the foundation for the numerical methods of "wave-tracing." Special thanks to John Sinton and Thom Cavanaugh for their guidance and cooperation.

REFERENCES

Aki, K., and Richards, P., 1980, Quantitative seismology: W. H. Freeman and Co., v. 2, 727-728.

Berryman, J. G., 1989, Stable iterative reconstruction algorithm for nonlinear traveltime tomography: Lawrence Livermore National Laboratory, internal report.

Harlan, W. S., 1989, Tomographic estimation of seismic velocities from reflected raypaths, Ann. Internat. Mtg., Soc. Expl. Geophys., Expanded Abstracts, 922-924.

Hagedoorn, J. G., 1954, A process of seismic reflection interpretation: Geophysical Prospecting, 2, 85-127.

Luenberger, D. G., 1984, Linear and nonlinear programming: Addison-Wesley Publ. Co., Inc.

Langen, R. T., Lerche, I., and Cutler R. T., 1985, Tracing of rays through an heterogeneous media: An accurate and efficient procedure: Geophysics, 50, 1456-1465.

Moser, T. J., 1989, Efficient Seismic Ray Tracing Using Graph Theory: SEG expanded abstracts, 1989 Internat'l Meeting and Expos., 1106-1108.

Scales, J. A., 1987, Tomographic inversion via the conjugate gradient method: Geophysics, 52, 179-185.

van Trier, J., and Symes, W. W., 1990, Upwind finite-difference calculations of traveltimes: Stanford Exploration Project, 65, 41-58.

Vidale, J. E., 1989, Finite-difference calculation of traveltimes in 3-D: SEG expanded abstracts, 1989 Internat'l Meeting and Expos., 1096-1098.

Wesson, R. L., 1971, Travel-time inversion for laterally inhomogeneous crustal velocity models: Bull. of the Seis. Soc. of Am., 61, 729-746.

Woodward, M. J., 1989, Wave-equation tomography: Ph.D. Thesis, Stanford Univ.

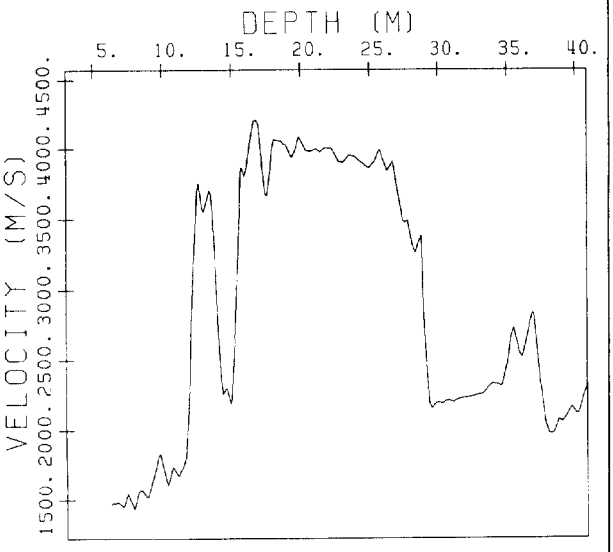

FIG. 1. A compressional (sonic) velocity log from the well containing receivers.

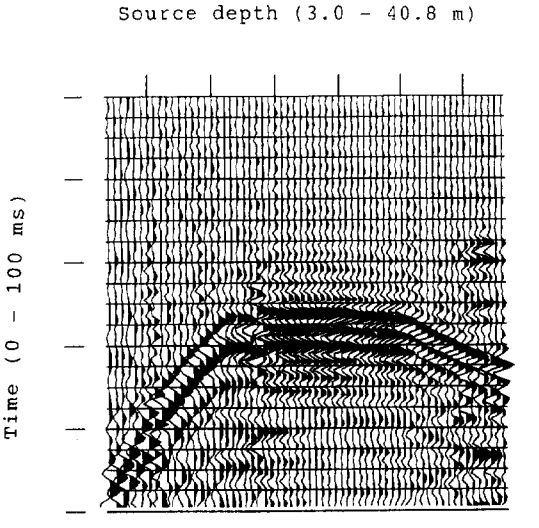

FIG. 2. A common-receiver, shear-wave gather for a receiver at 38.3 m depth. Traces show deconvolved recorded waveforms (0 to 100 ms) from 63 sources in a well 88.6 m away, increasing in depth (3.0 m - 40.8 m) from left to right.

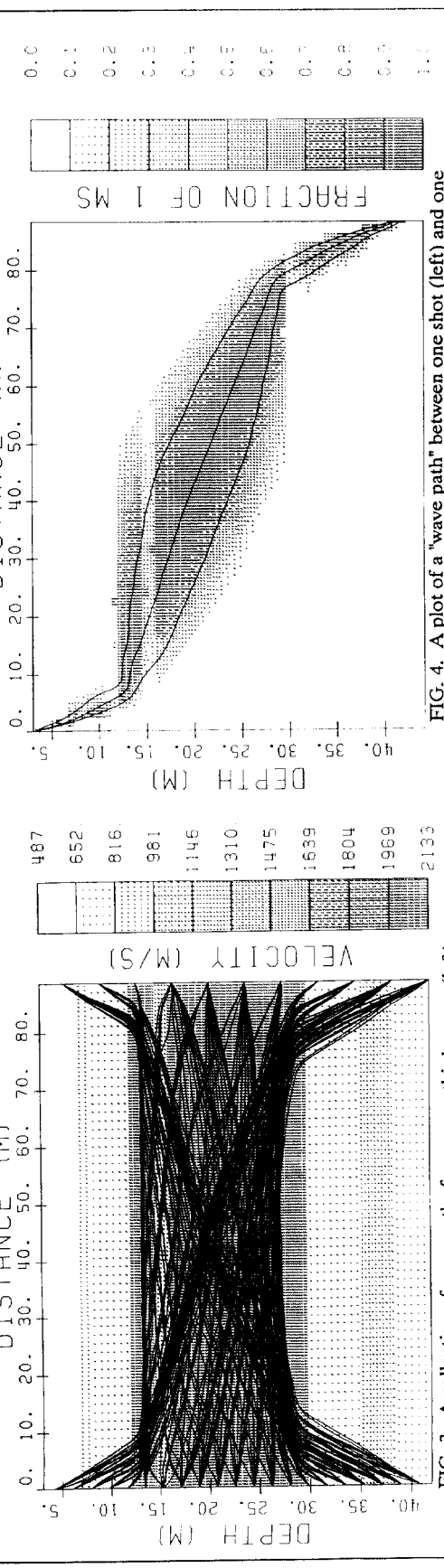

FIG. 3. A collection of wave paths from every third source (left) to all receivers (right). Note that all paths pass directly or are refracted through a high-velocity limestone. Most of the low-velocity shales are not covered by first arrivals.

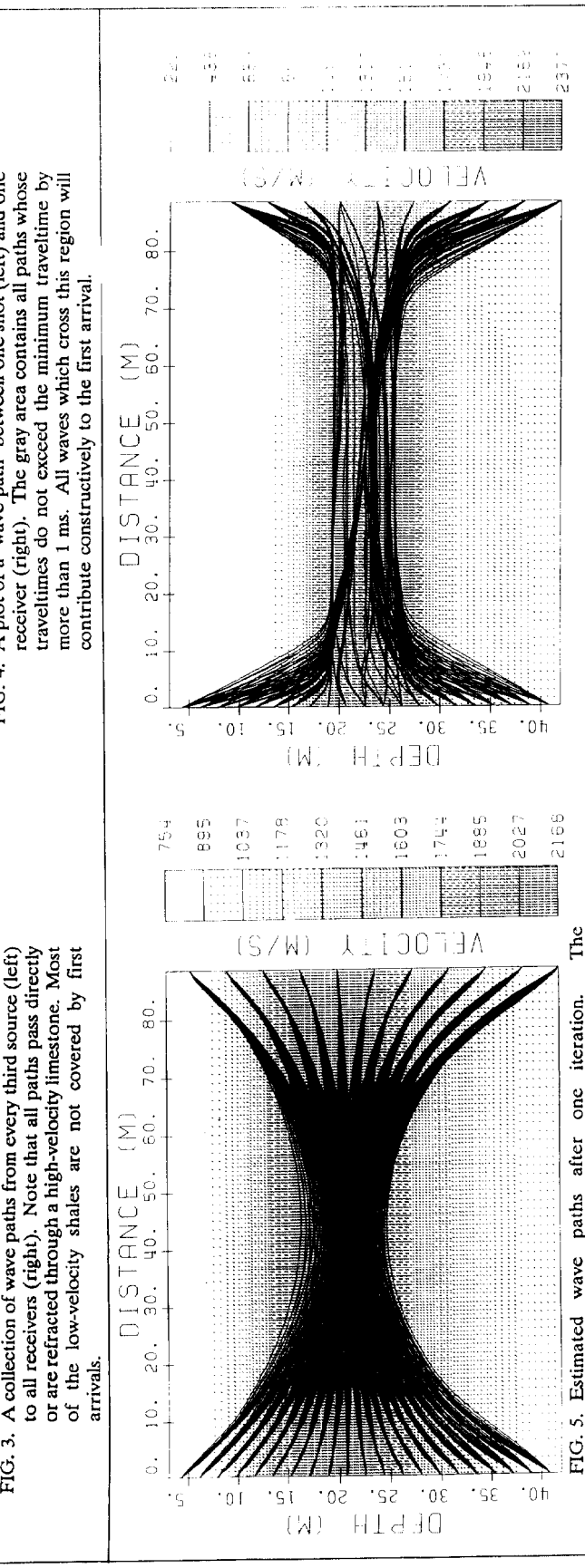

FIG. 5. Estimated wave paths after one iteration. The background shows the smooth velocity model estimated first from straight raypaths. The velocity function was allowed to change more rapidly with depth after each iteration.

FIG. 4. A plot of a "wave path" between one shot (left) and one receiver (right). The gray area contains all paths whose traveltimes do not exceed the minimum traveltime by more than 1 ms. All waves which cross this region will contribute constructively to the first arrival.

FIG. 6. The estimated two-dimensional velocity model and corresponding wavepaths.